Increased air pollution exposure among the Chinese population during the national quarantine in 2020

Huizhong Shen[a,b], Guofeng Shen[b,1], Yilin Chen[a], Armistead G. Russell[a], Yongtao Hu[a], Xiaoli Duan[c], Wenjun Meng[b], Yang Xu[b], Xiao Yun[b], Baolei Lyu[d], Shunliu Zhao[e], Amir Hakami[e], Shu Tao[b], Kirk R. Smith[f,1]

[a]School of Civil & Environmental Engineering, Georgia Institute of Technology, Atlanta, GA 30332, USA

[b]College of Urban and Environmental Sciences, Laboratory for Earth Surface Processes, Sino-French Institute for Earth System Science, Peking University, 100871 Beijing, China

[c]School of Energy and Environmental Engineering, University of Science and Technology Beijing, Beijing 100083, China

[d]Huayun Sounding Meteorology Technology Corporation, Beijing, 100081, China

[e]Department of Civil and Environmental Engineering, Carleton University, Ottawa, ON K1S 5B6, Canada

[f]Environmental Health Sciences, School of Public Health, University of California, Berkeley, CA 94720-7360, USA

[1]To whom correspondence may be addressed. Email: gfshen12@pku.edu.cn; krksmith@berkeley.edu

Short title: The COVID-19 quarantine increased $PM_{2.5}$ exposure in China.

Abstract

The COVID-19 quarantine in China is thought to have been beneficial for reducing the population exposure to ambient air pollution. The overall exposure also depends, however, on indoor air quality and human mobility and activities, which also changed during the pandemic. Here we integrate real-time mobility data, questionnaire survey on during-pandemic human activity patterns, advanced air quality modeling techniques, and an indoor exposure model. We first show a decrease of 16.7 $\mu g \cdot m^{-3}$ in the national average population-weighted ambient $PM_{2.5}$ during the quarantine (i.e., the one month following the start of the Spring Festival holiday). The total population-weighted exposure (PWE) to $PM_{2.5}$ considering both indoor and outdoor environments, however, increased by 5.7 $\mu g \cdot m^{-3}$. The increase in PWE was mainly due to the nationwide population migration from urban to rural areas before the Spring Festival coupled with the freezing of the migration backward due to the quarantine (+10.8 $\mu g \cdot m^{-3}$), which increased household energy consumption and the fraction of people exposed to rural household air pollution (HAP) indoors. The changes in PWE due to the quarantine were -14.0 and +19.2 $ug \cdot m^{-3}$ among urban and rural populations, respectively, and ranged from -9.1 $ug \cdot m^{-3}$ in the provinces with the highest per-capita income to 7.1 $ug \cdot m^{-3}$ in the provinces with the lowest. HAP contributed 82% of PWE during this period, which was likely more severe than any period in recent years. Our analysis reveals an increased inequality of air pollution exposure during the COVID-19 quarantine and highlights the importance of HAP for population health in China.

Introduction

Due to the outbreak of COVID-19, China activated the First Level Public Health Emergency Response (FLPHER, here called a quarantine), which required local governments to carry out strict restrictions on travel (1, 2). The entire country was under this quarantine, which lasted for one month and was arguably unprecedented regarding its spatial coverage, duration, strictness, and effectiveness for preventing the spread of COVID-19 (2). There was an observed improvement in ambient air quality during the quarantine likely due to the limited industrial and transportation activities coupled with favorable meteorological conditions (3-8). Some expected that the air quality improvement may have reduced the exposure of the population to air pollutants, such as NO_2 (6, 7, 9). If coupled with reductions in the ambient levels of fine particulate matter with a diameter smaller than 2.5 μm ($PM_{2.5}$) for which the best information is available on health impacts, the quarantine may have yielded an inadvertent health benefit during the COVID-19 pandemic. How actual population exposure changed, however, depends not only on the ambient air quality but also on the air quality indoors, and the mobility and daily activity patterns of individuals, such as the time spent in different locations (10-13).

The quarantine triggered by the outbreak started from Jan. 25, 2020, which coincided with the start of the 2020 Spring Festival. Just before the start, reportedly 125 million migrant workers had moved from urban to rural areas to reunite with their families (14). Normally, they would have returned at most one month after the start of the Festival (15). Such a nationwide returning-to-work tide, however, was frozen by travel restrictions under the quarantine (16, 17). Thus, an extra 9% of the Chinese population were kept in rural areas longer because of the COVID-19 outbreak, where household air pollution (HAP) is more severe due to the prevalent use of solid fuels (i.e., coal and biomass) for cooking (13, 18). Also, during that season, there was still significant space heating in households over much of the country, which is even more likely to be done with solid fuels than cooking (19).

The question we ask is how the overall $PM_{2.5}$ exposure of the Chinese population changed during the COVID-19 quarantine, taking into account the changes in indoor and outdoor concentrations, time spent indoors and outdoors, and large-scale migration patterns. Such an assessment is of interest because of the health impacts of short-term exposure to PM$_{2.5}$ (20-22) and the reported associations between PM$_{2.5}$ and the spread and severity of the COVID-19 infection (23, 24). Here we use real-time migration data, during-pandemic activity survey data, national census data, advanced air quality modeling techniques, and an indoor exposure model to track the dynamic changes in the population exposure to PM$_{2.5}$ across China before and during the nationwide quarantine (Materials and Methods).

Results and Discussion

Overall change in PM$_{2.5}$ exposure before and after the COVID-19 quarantine. We focus our comparison on two periods—P1, one month preceding the Spring Festival spanning from Dec. 25, 2019 to Jan. 24, 2020, and P2, one month following the start of the Spring Festival, i.e., the quarantine period, spanning from Jan. 25, 2019 to Feb. 25, 2020 (Figure 1). Using surveys on time-activity patterns of the Chinese population both in normal days and during the quarantine, population time use is parsed between indoors and outdoors (Materials and Methods). Data fusion using an ensemble deep learning method to integrate the ground-level measurements of the national monitoring network with the outputs of a chemical transport model (25) (Materials and Methods) shows a decrease of 16.7 ug·m^{-3} (15.3–18.2 ug·m^{-3}, uncertainty is expressed as 95% confidence interval throughout) in the population-weighted average of ambient (outdoor) PM$_{2.5}$ concentrations between P1 (64, 58–69 ug·m^{-3}) and P2 (47, 43–51 ug·m^{-3}). In contrast, the population-weighted exposure (PWE) that considers both indoor and ambient concentrations shows an increase of 5.7 ug·m^{-3} (4.2–8.2 ug·m^{-3}) in P2 (101, 84–122 ug·m^{-3}) compared to P1 (95, 79–114 ug·m^{-3}) (Figure 1), suggesting important roles of other factors, including population migration and the time spent indoors, in the PWE change under the quarantine. Decomposition analysis, by changing the factors severally, attributes the changes of -10.5 (-11.0–-9,3), 10.8 (7.4–15.0), and 5.4 (4.3–6.9) ug·m^{-3} in PWE to the changes in ambient PM$_{2.5}$, population migration, and time spent indoors, respectively (Figure 2). Note that changes in ambient PM$_{2.5}$ affect indoor concentration through infiltration, which is included in our assessment. Population migration alone offsets the effect of the ambient air quality improvement on PWE (10.8 due to migration vs. -10.5 $ug \cdot m^{-3}$ due to ambient air) (Figure 2).

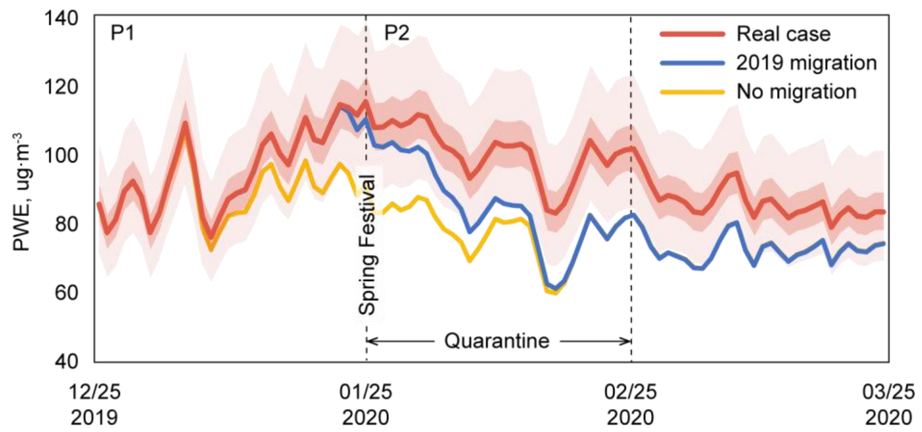

Figure 1. Daily trends of PWE in the real case and under different counterfactual scenarios during the study period. The dark and light shaded areas represent the inter-quartile range and the 95% confidence interval of the real-case time series, respectively. Compared to the real case, the "2019 migration" scenario assumes that there was no COVID-19 outbreak such that the migration followed the pattern of the 2019 Spring Festival (instead of 2020) and the time spent indoors was not affected by the quarantine. The "no migration" scenario assumes no COVID-19 outbreak and no Spring Festival migration. Ambient $PM_{2.5}$ levels remain the same across the scenarios. The difference between the real case and the "2019 migration" scenario reflects the impacts of the quarantine-induced freezing of the migration and the change in time spent indoors on PWE. The difference between the "2019 migration" and "no migration" scenarios reflects the impact of the Spring Festival migration on PWE in normal year.

The effects of migration on PWE. The dynamic cross-province migration dataset we established is based on the national census data (26) and official reports (14) and is temporally allocated using the Baidu real-time mobility data (27) (Materials and Methods). The direction of the migration is characterized on a province-to-province basis and further divided into four categories: 1) urban-to-rural, 2) urban-to-urban, 3) rural-to-rural, 4) rural-to-urban. The migration started about 25 days before the Spring Festival and had two phases with opposite directions—one occurred in P1, the other in P2. Before the Spring Festival (P1), there were estimated 236 million people returning to their hometowns, accounting for one sixth of the total population. Urban-to-rural migration contributed 53% of the total, of which the majority were reportedly rural migrant workers (14). Urban-to-urban migration contributed 34%, and other two types of migration were relatively minor (10% for rural-to-rural, 3% for rural-to-urban). After the Spring Festival (P2) when people would normally move back to cities, however, the nation was under quarantine in response to the outbreak of COVID-19, and the migration froze. The effect of the quarantine on the migration in P2 is clearly illustrated by the day-by-day comparison in the migration intensity in 2020 with the previous year (Figure 3). The migration in P2 was close to completion within 25 days after the 2019 Spring Festival, by which time this year the migration was only 18% complete (Figure 3).

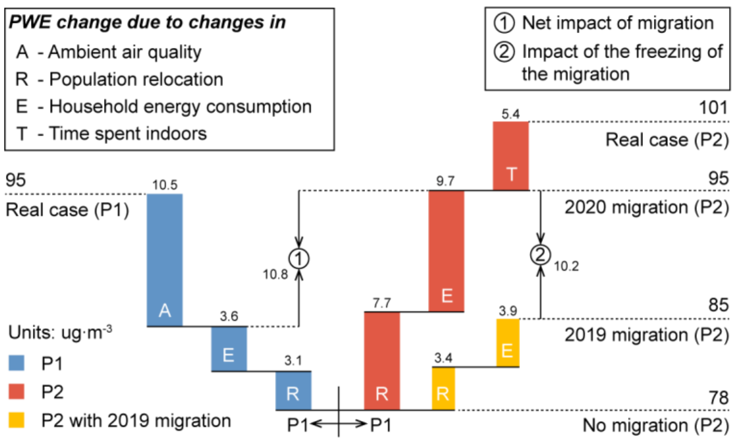

Figure 2. Decomposition analysis of the PWE change between P1 and P2. The overall change in the PWE of the Chinese population is decomposed into the changes in PWE due to the changes in ambient air quality, population relocation, household energy consumption, and time spent indoors. Note that the migration had two phases with opposite directions—the first one (during P1) preceded the Spring Festival when people returned to their hometowns, the second (during P2) followed the first as people traveled back to work. The quarantine froze the second phase of the migration, leading to a net difference in the migration impact on PWEs between P1 and P2, as marked in the figure. The impact of the quarantine-induced freezing of the migration in response to COVID-19 in P2 are evaluated by comparing with the PWE under 2019 migration pattern and are also marked in the figure. PWEs are in μg·m^{-3}.

The migration led to a shift in the fraction of population residing in rural areas. The fraction reached its maximum of 47.6% during the Spring Festival as did in normal years but decreased at a pace one seventh the pace of normal years afterwards due to the quarantine (0.05% per day in 2020 vs. 0.34% per day in 2019) (Figure 3).

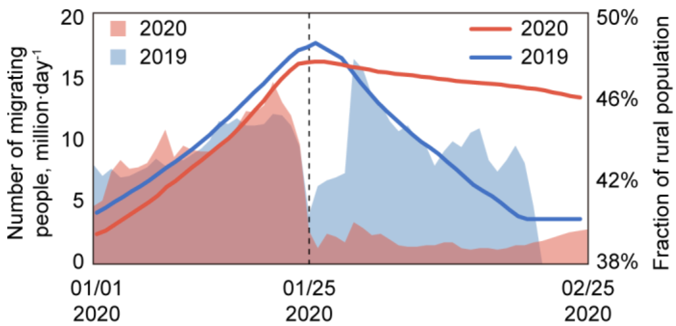

Figure 3. The population migration around the Spring Festivals of 2019 and 2020. The shaded areas illustrate the temporal trend of the number of people migrating each day. The solid lines show the temporal trends of the fraction of rural population (i.e., the population residing in rural areas) in the total population. The black dashed line marks the Spring Festival. The x-axis represents the calendar date in 2020.

Two main consequences of such a change in the migration for population exposure were 1) an larger fraction of people exposed for a longer time to HAP in rural households which is usually more severe than in urban households (13, 18) and 2) increased rural energy consumption to meet the demand of the immigrants, both of which further worsened HAP. Based on a recently conducted national survey on rural household energy consumption (19) and the indoor exposure model (10, 12) (Materials and Methods), we estimate that by increasing the fraction of rural population, the migration enhanced the nationwide PWE by 3.1 and 7.7 ug·m^{-3} in P1 and P2, respectively, compared to a baseline scenario assuming no migration (Figure 2), while by increasing the household energy consumption, the migration further increased the PWE by 3.6 and 9.7 ug·m^{-3}, respectively, in P1 and P2 (Figure 2). This amounts to the total increases of 6.6 and 17.4 ug·m^{-3} in PWE in P1 and P2, respectively. To isolate the impact of the COVID-19-induced freezing of the migration on PWE, we substitute 2019's migration for that experienced in 2020 while keeping all other factors equal (i.e., outdoor air quality, time spent indoors, baseline energy mix, etc.). The results show a comparable increase in PWE in P1 (6.5 ug·m^{-3} in 2019 vs. 6.6 ug·m^{-3} in 2020) but a much smaller increase in P2 (7.2 vs. 17.4 ug·m^{-3}), suggesting an enhancement of 10.2 ug·m^{-3} (17.4 minus 7.2) in PWE due to the freezing of the migration under the national quarantine.

The contribution of HAP on PWE and the inequality of the PWE change. Focusing on the quarantine period (P2), we consider the changes in HAP and other sectors (i.e., transportation, industry, and power generation) and assess the overall impacts of the quarantine on indoor and ambient air quality and on PWE. Our assessment shows an estimated decrease of 15.6 (8.6–22.6) ug·m^{-3} in the population-weighted average ambient $PM_{2.5}$ due to the quarantine, which is similar in magnitude to the $PM_{2.5}$ reduction before and after the COVID-19 outbreak (16.7 ug·m^{-3}) (Figure 4). We note, however, that unlike our fused $PM_{2.5}$ field which is the best guess of the real-world $PM_{2.5}$ concentrations, our impact assessment on ambient $PM_{2.5}$ using chemical transport model is limited by the uncertainty in the estimation of quarantine-induced emission reduction (Material and Methods) and the capability of the model to reproduce the actual $PM_{2.5}$ change in response to the emission reduction (28), both of which warrant further investigation. The indoor $PM_{2.5}$ concentration is estimated to increase by 3.1 (2.4–3.8) ug·m^{-3} due to the quarantine (Figure 4B) which is a result of the competition between the exacerbation of HAP (12.2 ug·m^{-3}) and the improvement in ambient $PM_{2.5}$ that infiltrates indoors (-9.1 ug·m^{-3}). Incorporating the changes in indoor and ambient $PM_{2.5}$ with population migration and human activities, we estimate that the COVID-19 quarantine led to a net increase of 5.9 (4.5–7.3) ug·m^{-3} in PWE (Figure 4B).

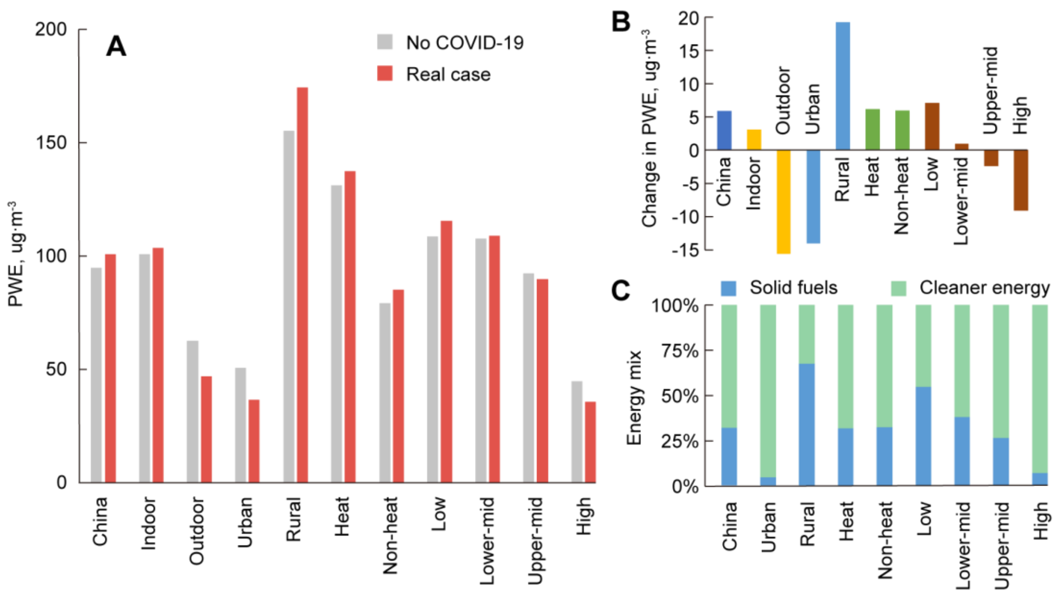

Figure 4. The impacts of the responses to COVID-19 on PWEs and the use of solid fuels as a driving factor. The PWEs in the real case and in the no-COVID-19 scenario (**A**), the changes in PWEs due to the responses to COVID-19 (**B**), and the shares of solid fuel use in household energy mix (**C**) in China, in indoor/outdoor environments, in urban/rural areas, in heating/non-heating regions, and in provinces with different per-capita income levels. The shares of solid fuel use in household energy mix in indoor/outdoor environments are the same as in national total, and thus are not shown in **C**.

We calculate the contribution of HAP on PWE, which includes the direct contributions to indoor and outdoor $PM_{2.5}$ and the indirect contribution of outdoor HAP to indoor $PM_{2.5}$ through infiltration (Figure S1). HAP dominated the PWE in P2 regardless of whether there was a quarantine, whereas the COVID-19-induced quarantine increased the HAP contribution on PWE from 74% (no quarantine or no COVID-19) to 82% (in the real case) (Figure S2).

The contribution of HAP to PWE during this period was higher than that before the COVID-19 quarantine (68%), or in a counterfactual scenario where there was no migration (70%), or for annual average (62%) (Figure S2). The leading cause of HAP is the use of solid fuels (e.g., coals and biomass) for cooking and heating, which is much more prevalent in rural areas (67.5% as the share of solid fuels in the household energy mix) than in urban areas (4.7%) (Figure 4C). Further investigation shows a clear tendency toward a stronger positive effect of the quarantine on PWE as the share of solid fuel use increased (Figure 4B and C and Figure S3) and that the PWE in rural areas was estimated to increase by 19.2 $ug{\cdot}m^{-3}$ due to the quarantine, while the urban PWE decreased by 14.0 $ug{\cdot}m^{-3}$.

The change in exposure associated with solid fuel use and the contrary changes in rural and urban PWEs are due primarily to the interaction between HAP and the human activities: the longer time spent indoors during the pandemic increased the time length for people being exposed to HAP and thus increased the PWE among rural residents; the freezing of the migration in the meanwhile increased the rural household energy consumption and subsequently increased the severity of HAP. On the other hand, in urban areas where indoor air quality is often better than outdoor (29), the increase in the time spent indoors reduced PWE.

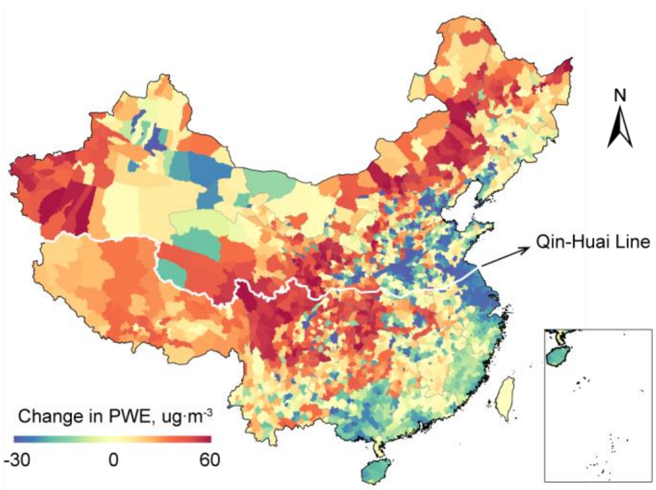

Figure 5. The spatial distribution of the changes in PWE among the Chinese population due to responses to COVID-19. Changes in ambient and indoor air quality, population migration, and time spent indoors are considered. The PWE changes are illustrated by county. The white line marks China's Qinling Mountains-Huai River Line (Qin-Huai Line) Qin-Huai Line divides China into two regions that differ in climate and is commonly used as a reference line in policy making to determine the heating (northern) and non-heating (southern) regions (30).

The association between PWE and HAP led to the spatial heterogeneity (Figure 5) and population inequality in the quarantine-induced changes in PWE (Figure 4C) which ranged from -19.0 $ug \cdot m^{-3}$ in Tianjin to 32.5 $ug \cdot m^{-3}$ in Inner Mongolia and from -9.5 $ug \cdot m^{-3}$ in the provinces with average per-capita incomes higher than 5000 USD to 6.5 $ug \cdot m^{-3}$ in the provinces with average per-capita incomes lower than 3000 USD, suggesting inequal changes in PWE by income group. The inequality in the PWE changes is further confirmed by the significant negative correlation between the PWE changes and provincial per-capita income levels ($p = 2 \times 10^{-4}$) and survives the assessments using county-level data or focusing on the rural population exclusively (Figure S4A and B).

The urban population does not show significant inequality (Figure S4C) likely due to the much less dependence on solid fuels and therefore being less affected by HAP than their rural counterparts. Regression analysis reveals a significant interaction between the per-capita income and the epidemic severity in the model to predict the quarantine-induced changes in PWE and suggests that regions with more severe epidemic situation are associated with greater inequality. In Hubei, every 20% reduction in income is estimated to be associated with a 6.7 $ug \cdot m^{-3}$ increase in PWE due to the quarantine, which is almost twice the increase (3.4 $ug \cdot m^{-3}$) for the national average (Figure S4A).

The effect of Clean Heating Plan on the PWE changes. Despite the heterogeneity and inequality, the quarantine-induced increases in PWE in the heating (north) and non-heating (south) regions are found to be comparable (6.2 and 5.9 $ug \cdot m^{-3}$ in heating and non-heating regions, respectively) (Figure 4B and Figure 5). We find that a recently implemented campaign called “Clean Winter Heating Plan in Northern China” (“Clean Heating Plan” for short), played an important role in balancing the PWE increases between heating and non-heating regions. Clean Heating Plan was launched by the Chinese central government in 2017 and set stringent and differentiate goals through 2021 toward a high rate of clean heating (i.e., the rate of clean energy used for heating) in the northern region, with the rates ranging from 40% in rural areas to 100% in some major cities (31). This campaign, if successfully implemented, would reduce the amount of annual coal consumption by 150 Tg, and recent progress has shown much success in the implementation of this campaign such that it is expected to be achieved ahead of schedule (32).

We estimate that Clean Heating Plan had phased out 44.4% of the solid fuels used in households in the Northern provinces by the end of 2019. If there was no such a campaign, we estimate that the COVID-19-induced increase in PWE would be almost doubled in the heating region (12.0 $ug \cdot m^{-3}$). In addition, the population inequality in the PWE increase, measured by the increase in PWE per 20% reduction in income, would be 30.1% higher than is estimated in the real case (4.6 vs. 3.5 $ug \cdot m^{-3}$) in the heating region (Materials and Methods). In an ideal case where Clean Heating Plan was fully phased in, the quarantine would only lead to an increase of 2.3 $ug \cdot m^{-3}$ in PWE in the heating region, with the inequality decreased by 15.6%. Our analysis thus reveals that Clean Heating Plan moderated the quarantine-induced increases in PWE in the heating region, reduced the inequality of the PWE increases among different income groups of people, and put the PWE increases of the heating and non-heating regions in the balance. Still, the PWE in the heating region (137 $ug \cdot m^{-3}$) was 61% higher than was in the non-heating region (85 $ug \cdot m^{-3}$), and the quarantine-induced increase in rural PWE in the heating region (24.4 $ug \cdot m^{-3}$) was 31% higher than was in the non-heating region (18.6 $ug \cdot m^{-3}$).

Conclusion. In this study, we integrate multiple data sources and modeling techniques to dynamically track the changes in PWE due to the national quarantine. We first show that the national population-weighted exposure to ambient $PM_{2.5}$ reduced by 16.7 $ug \cdot m^{-3}$. This is approximately a 26% drop compared to the 40–60% drop reported widely (4, 8, 33, 34) for ambient NO_2 levels (not populations-weighted) measured by ground-level monitors and satellites. This difference is apparently due to the different emission source characteristics of the two pollutants, with NO_2 coming mainly from vehicles and industry (35), which were substantially curtailed during the quarantine (28). A much greater proportion of $PM_{2.5}$, on the other hand (36), comes from household fuels use of which probably grew during the quarantine.

We show that, the average PWE of the population is estimated to increase despite a decrease in ambient $PM_{2.5}$, which is mainly due to the worsened HAP and a higher opportunity for people to be exposed to HAP during the pandemic. Changes to the actual dose of $PM_{2.5}$ to the population of course, will also depend on changes in use and effectiveness of facemasks during the period.

With respect to the distribution of PWE, our assessment reveals an increase in the environmental inequality of air pollution exposure in response to the COVID-19 crisis. While the high-income group benefited from the reduction of PWE, the low-income group suffered a significant increase in PWE. Such inequality would be even higher if Clean Heating Plan that targets HAP in the northern China was not implemented. In addition, given the reported association between short-term exposure to air pollution and the transmission of COVID-19 (23), this analysis shows how the COVID-19 pandemic itself as well as the quarantine may have deepened health inequalities. Our assessment highlights the importance of mitigating HAP for reducing the environmental inequality and protecting human health. If society is to confine people to their homes for their protection, it is far better that they are clean to start with.

Methods and Materials

Household energy consumption

Provincial-level household energy consumption data were collected and compiled based on a representative national survey (19) and China Statistical Yearbook (43). The data were downscaled to county level and extrapolated to 2020 (the study year) based on the fuel-type-specific empirical models developed by Shen et al. (38). Following a previous study (10), the clean heating targets set by Clean Heating Plan were incorporated into the energy trends in the heating region.

Migration data

We derived detailed origin and destination information from the 6th National Census (26) to characterize population migration on the county level (38). The census data classified the migrants into four groups—rural-to-urban, urban-to-urban, rural-to-rural, and urban-to-rural, and are representative of the migration pattern in 2010. The census data showed a total of 138 million migrant workers in 2010, noting that not all the migrants intended to return home during the Spring Festival holidays. The Ministry of Human Resources and Social Security reported 125 million migrant workers returning home in 2020 (14). Therefore, the census data was scaled down by a factor of 0.9 to represent the migration pattern in 2020. We assumed that all the back-home migrations were achieved before the second day of the Spring Festival holidays, and that the returning-to-work migration started from the first day of the Spring Festival holidays. The migration flows (i.e., the number of migrants) were temporally allocated using the daily cross-province mobility intensities reported by the Baidu real-time mobility monitoring platform as a surrogate (27). For the 2019 Spring Festival of which the detailed provincial-level Baidu mobility data were not available, the national-level mobility intensities were used to scale the 2020 migration pattern to 2019, assuming that the relative difference in the migration flows across provinces remained unchanged between 2019 and 2020.

Survey on human activity pattern

The information on the daily time spent indoors and in different indoor compartments (i.e., kitchen, living room, and bedroom) in wintertime were derived from Exposure Factors Handbook of Chinese Population (39), as summarized by Chen et al. (12), and were used in this study to represent the time-activity pattern when there was no COVID-19. The time-activity pattern during the pandemic were derived from an online questionnaire survey (https://www.wjx.cn/m/59666734.aspx) which collected information on the frequencies of going out during the quarantine. This survey adopted strict quality control measures during data processing and analysis. The questionnaires with missing values, logical errors and data format errors were excluded. Two groups of personnel independently derived the data and completed the comparison to ensure the accuracy of the results. 8330 questionnaires were distributed with a recovery rate of 100%. A total of 7784 valid questionnaires were obtained, covering 31 provinces in China. The survey showed that the more severe the epidemic, the less frequently people went out each day. The frequency data were translated into the time length of outdoor stay by assuming time lengths for each going-out event ranging from 200 minutes per time in the provinces that were the least affected by the COVID-19 outbreak (i.e., Qinghai and Tibet) to 120 minutes per time in Hubei where the outbreak was the most severe. The uncertainty induced by this assumption was considered in the uncertainty analysis specified in following section. The average time spent indoors by province before and during the pandemic was summarized in Table S1.

Emissions and air quality modeling

We used AiMa emission inventory (41, 42) as the emission input to conduct the air quality modeling for ambient $PM_{2.5}$ assessment. The emission inventory has been compiled by integrating a variety of inventories and activity data (42) and has undergone continuous updates. This inventory is currently used by an online operational system (called "AiMa" system) that provides air quality forecast for government and public (http://www.aimayubao.com/). The base year of the latest version of AiMa inventory is 2017.

The ambient $PM_{2.5}$ concentrations were obtained by combining hourly ground-level observations reported by the China National Urban Air Quality Real-time Publishing Platform (5) with model predictions by the Community Multiscale Air Quality (CMAQ) model (44) using an ensemble deep learning data fusion approach (25). Meteorological variables were derived from the AiMa system, which were generated by the Weather Research Forecasting (WRF) model version 3.4.1 (45) driven by the 0.5-degree global weather forecast products produced by the National Centers for Environmental Prediction Global Forecast System (46). The downscaled meteorology together with the AiMa emission inventory was used to drive CMAQ simulation which was conducted to cover the mainland China on a horizontal resolution of 12 km with 13 vertical layers extending up to ~16 km above ground. The model output was fused with observations to get the final ambient $PM_{2.5}$ concentration fields across China on a daily resolution over the study period (i.e., from Dec. 25, 2019 to Mar. 25, 2020). More details about the emission inventory, the model configuration, the data fusion approach and its performance can be found in a previous study (25).

We conducted adjoint analysis to decompose the contributions of various emission sources to outdoor $PM_{2.5}$ concentrations. The emission sources, as categorized in the AiMa inventory, included power generation, industry, residential (i.e., household), transportation, agriculture, solvent usage, fugitive dust, and fires. CMAQ-Adjoint version 5.0 (40) was applied to calculate the adjoint sensitivities. The adjoint analysis provides location- and time-specific gradients (i.e., adjoint sensitivities) and can be used in applications such as backward sensitivity analysis, source attribution, optimal pollution control, data assimilation and inverse modeling (40). The CMAQ-Adjoint version 5.0 is the most up-to-date version of CMAQ-Adjoint. Discrete adjoint is implemented for gas-phase chemistry, aerosol formation, cloud chemistry and dynamics, and diffusion. Continuous adjoint is implemented for advection. The model performance has been comprehensively evaluated in the previous study (40), showing good agreements with the results given by forward sensitivity analysis.

In this study, the cost function of the adjoint analysis was defined as the ambient population weighted average $PM_{2.5}$ concentration over the study period across China. The adjoint model thus provided sensitivities of this cost function to per-unit emissions of various species in each model grid cell. Using the source-specific emission information, we evaluated the source contributions of household (i.e., residential) energy consumption and other sectors on ambient air pollution by province. Details about the principle equations, development, and evaluation of CMAQ-Adjoint can be found in previous studies (40, 47).

Using the adjoint sensitivities, we further evaluated the changes in the population-weighted concentration in response to the emission reduction during the quarantine. Following previous study (28), we assumed a reduction of 10% in power plant emissions, 30% in industrial emissions, and 70% in mobile emissions. The changes in residential emissions due to population migration were evaluated using the procedures as specified in our previous studies (37, 38).

Indoor exposure model

We employed an indoor exposure model developed by Chen et al. (12) to quantify the indoor $PM_{2.5}$ levels. The model was modified to take into account the change in the amount of household energy consumption and outdoor infiltration and to unify the estimation approach for urban and rural household conditions as follows,

$$C_{in} = C_{in,add} + C_{out,add} \quad (1)$$

where C_{in} is the indoor $PM_{2.5}$ concentration in $\mu g \cdot m^{-3}$, $C_{in,add}$ is the C_{in} component contributed by indoor sources, and $C_{out,add}$ is the C_{in} component contributed by outdoor infiltration. $C_{in,add}$ was calculated by the following equation,

$$C_{in,add} = \frac{\sum E_f \cdot C_{f,k} \cdot T_k}{\bar{E} \cdot \sum T_k} \quad (2)$$

where subscripts f and k denote the type of fuel (i.e., wood, straw, coal, and cleaner energy) and indoor compartment (i.e., kitchen, living room, and bedroom), respectively; E_f is the per-household daily consumption of fuel type f in terms of thermal energy amount (i.e., the amount of energy consumption after thermal efficiency conversion); $\bar{E}$ is the average per-household daily thermal energy required for cooking and heating; $C_{f,k}$ is the $C_{in,add}$ in indoor compartment k when $E_f = \bar{E}$ and the household consumes fuel f solely; T_k is the time spent daily in indoor compartment k. Following a previous study (48), the thermal efficiencies of biomass, coal, gas, and electricity are 0.154, 0.244, 0.555, and 0.84, respectively. $\bar{E}$ values 40 MJ·day^{-1}·household^{-1} which was calculated as the national average daily household thermal energy consumption for cooking and heating in winter. $C_{f.k}$ values were adopted from a previous study (12) in which the means and variations of $C_{f.k}$ were determined by mete-analysis through literature review. The mean heating-season $C_{f.k}$ in kithen/living room are 283, 434, and 547 μg·m^{-3} for coal, crop, and wood, respectively, and in bedroom are 211, 267, 359 μg·m^{-3} for coal, crop, and wood, respectively. Cleaner energy was assumed to cause little addition to indoor $PM_{2.5}$, and thus the $C_{f.k}$ for cleaner energy was set to be 0. Equation (2) assumes that with all others equal, $C_{in,add}$ is proportional to the thermal amount of daily energy consumption of the household. This assumption was testified and supported by sensitivity tests using a single-box model (49), as recommended in World Health Organization's indoor air quality guidelines (50), to predict $C_{in,add}$ based on varying amounts of energy consumption. $C_{out,add}$ was calculated by multiplying ambient $PM_{2.5}$ concentrations with region-specific infiltration factors following Xiang et al.'s method (51). The $PM_{2.5}$ exposure of individuals at a specific location was calculated as the average of the indoor and outdoor $PM_{2.5}$ concentrations weighted by the time fractions of indoor and outdoor stays. The PWE in a region was calculated as the population-weighted average of the individuals' exposure within this region. The same approach to calculate PWE has been adopted in previous studies (10, 11).

Regression analysis

We conducted regression analysis to predict the county-level quarantine-induced changes in PWE.

The regression showed significant interaction between per-capita income and the epidemic severity. The regression equation is as follows,

$$dPWE = -31.9 \times \ln(INC_{per}) - 0.69 \times SEV \times \ln(INC_{per}) + 124.6 \quad (3)$$

where *dPWE* denotes the change in PWE due to the COVID-19 induced quarantine, in ug·m^{-3}; INC_{per} is per-capita annual income, in USD; *SEV* is the epidemic severity determined by the confirmed cases in the provinces (Table S1), ranging from 1 in Qinghai and Tibet (the least severe) to 5 in Hubei (the most severe).

Uncertainty analysis

The uncertainty in the PWE estimates stemmed from various sources, including the uncertainties in the modeled ambient and indoor concentrations, population migration, and time-activity patterns. We conducted Monte Carlo simulation to propagate the uncertainties from the input variables to PWE. For most input variables (e.g., concentration, migration intensity, time spent indoors, etc.), we assumed log-normal distributions to avoid negative values and used geometric coefficient of variation (GCV) (52) to measure the uncertainty. GCV is defined as follows,

$$GCV = e^{\sigma} - 1 \quad (4)$$

where e^{σ} is the geometric standard deviation (53). According to the performance of the data fusion approach evaluated in a previous study which showed good agreement with an independent observation dataset (25), the GCV of the population-weighted average of the fused $PM_{2.5}$ concentrations was derived as 4.4%. Given the large uncertainty in the estimated emission reduction due to the responses to COVID-19, the GCV for the emission reduction was set to be 40%. The GCVs of the population migration intensity and the time spent indoors during the quarantine were assumed to be 20% and 10%, respectively. For the time spent indoors in normal days, GCV of 5% was used based on the method of Chen et al. (12). For $\bar{E}$, we assumed a uniform distribution with a variation interval of 20% which is usually applied to reflect the uncertainty in the statistics of household solid use (37, 54). The CVs of the infiltration factors in indoor/outdoor air exchange was set to be 12.5% following Shi et al. (55). The uncertainties in indoor $PM_{2.5}$ concentrations in households using solid fuels were derived by Chen et al. based on 1821 observations collected from the literature (12). Monte Carlo simulations were performed 1,000,000 times to propagate the uncertainties in these input variables into the uncertainty in PWE.

Data availability

The population distribution data, the daily cross-province migration data, the daily ground-level $PM_{2.5}$ fusion data, and all data used to generate the figures in the main text are openly available on Open Science Framework at https://osf.io/x46tb/.

Code availability

The CMAQ source code can be accessed at https://www.epa.gov/cmaq/how-cite-cmaq. Upon completion of expanded user testing, the CMAQ Adjoint code will be hosted and distributed by U.S. EPA.

Acknowledgements. We thank Haoran Xu, Wenxiao Zhang, Xinyuan Yu, Yu'ang Ren, and Weiying Hou for their help with the energy data collection and the indoor model development. This work is funded by the Chinese Academy of Science (XDA23010100), the National Natural Science Foundation of China (Grant 41830641, 41629101, 41991312, 41922057, and 41821005), the U.S. Environmental Protection Agency (EPA grant number R835880), and the National Science Foundation (NSF SRN grant number 1444745). Its contents are solely the responsibility of the grantee and do not necessarily represent the official views of the supporting agencies. Further, the US government does not endorse the purchase of any commercial products or services mentioned in the publication.

References

1. Xinhua News (2020) 30 provinces activated First-level Public Health Emergency Response, http://www.xinhuanet.com/politics/2020-01/25/c_1125502232.htm.
2. Tian H*, et al.* (2020) An investigation of transmission control measures during the first 50 days of the COVID-19 epidemic in China. *Science* 368(6491):638-642.
3. CNN News (2020) There's an unlikely beneficiary of coronavirus: The planet, https://edition.cnn.com/2020/03/16/asia/china-pollution-coronavirus-hnk-intl/index.html.
4. Bauwens M*, et al.* (2020) Impact of coronavirus outbreak on NO2 pollution assessed using TROPOMI and OMI observations. *Geophys. Res. Lett.*:e2020GL087978.
5. China National Environmental Monitoring Center (2020) China National Urban Air Quality Real-Time Publishing Platform. http://www.cnemc.cn/.
6. He G, Pan Y, & Tanaka T (2020) COVID-19, City Lockdowns, and Air Pollution: Evidence

from China. *medRxiv*. doi: https://doi.org/10.1101/2020.03.29.20046649.

7. Venter ZS, Aunan K, Chowdhury S, & Lelieveld J (2020) COVID-19 lockdowns cause global air pollution declines with implications for public health risk. *medRxiv*. doi: https://doi.org/10.1101/2020.04.10.20060673
8. Zhao Y*, et al.* (2020) Substantial Changes in Nitrogen Dioxide and Ozone after Excluding Meteorological Impacts during the COVID-19 Outbreak in Mainland China. *Environmental Science & Technology Letters* https://doi.org/10.1021/acs.estlett.0c00304.
9. Isaifan R (2020) The dramatic impact of Coronavirus outbreak on air quality: Has it saved as much as it has killed so far? *Global Journal of Environmental Science and Management* 6(3):275-288.
10. Meng WJ*, et al.* (2019) Energy and air pollution benefits of household fuel policies in northern China. *Proc. Natl. Acad. Sci. U. S. A.* 116(34):16773-16780.
11. Zhao B*, et al.* (2018) Change in household fuels dominates the decrease in PM2. 5 exposure and premature mortality in China in 2005–2015. *Proceedings of the National Academy of Sciences* 115(49):12401-12406.
12. Chen YL*, et al.* (2018) Estimating household air pollution exposures and health impacts from space heating in rural China. *Environ. Int.* 119:117-124.
13. Smith KR*, et al.* (2014) Millions dead: how do we know and what does it mean? Methods used in the comparative risk assessment of household air pollution. *Annu. Rev. Public Health* 35:185-206.
14. Central People's Government of the People's Republic of China (2020) *A press conference held by the Ministry of Human Resources and Social Security to introduce the progress of the human and social departments' work related to the epidemic*. http://www.gov.cn/xinwen/2020-03/19/content_5493239.htm
15. Ministry of Transport of the People's Republic of China (2020) *Big data: the travel volume predictions during Lunar New Year holiday in 2020*. http://www.mot.gov.cn/fenxigongbao/yunlifenxi/202001/t20200109_3322161.html
16. Kraemer MU*, et al.* (2020) The effect of human mobility and control measures on the COVID-19 epidemic in China. *Science* 368(6490):493-497.
17. Xinhua News (2020) Traffic system works well in the seventh day of the Spring Festival holiday, http://www.xinhuanet.com/politics/2020-01/30/c_1125514185.htm.
18. Zhang JJ & Smith KR (2007) Household air pollution from coal and biomass fuels in China: Measurements, health impacts, and interventions. *Environ. Health Perspect.* 115(6):848-855.
19. Tao S*, et al.* (2018) Quantifying the rural residential energy transition in China from 1992 to 2012 through a representative national survey. *Nature Energy* 3(7):567-573.
20. Di Q*, et al.* (2017) Association of short-term exposure to air pollution with mortality in older adults. *JAMA* 318(24):2446-2456.
21. Dominici F*, et al.* (2006) Fine particulate air pollution and hospital admission for cardiovascular and respiratory diseases. *JAMA* 295(10):1127-1134.
22. Katsouyanni K*, et al.* (1997) Short term effects of ambient sulphur dioxide and particulate matter on mortality in 12 European cities: results from time series data from the APHEA project. *BMJ* 314(7095):1658.
23. Yongjian Z, Jingu X, Fengming H, & Liqing C (2020) Association between short-term exposure to air pollution and COVID-19 infection: Evidence from China. *Sci. Total*

Environ.:138704. doi: 10.1016/j.scitotenv.2020.138704.
24. Wu X, Nethery RC, Sabath BM, Braun D, & Dominici F (2020) Exposure to air pollution and COVID-19 mortality in the United States. *medRxiv*. doi: https://doi.org/10.1101/2020.04.05.20054502.
25. Lyu B*, et al.* (2019) Fusion Method Combining Ground-Level Observations with Chemical Transport Model Predictions Using an Ensemble Deep Learning Framework: Application in China to Estimate Spatiotemporally-Resolved PM2. 5 Exposure Fields in 2014–2017. *Environ. Sci. Technol.* 53(13):7306-7315.
26. National Bureau of Statistics of the People's Republic of China (2011) Census Data. http://www.stats.gov.cn/tjsj/pcsj/.
27. Baidu Inc (2020) Baidu migration, https://qianxi.baidu.com/2020/.
28. Huang X*, et al.* (2020) Enhanced secondary pollution offset reduction of primary emissions during COVID-19 lockdown in China. doi: 10.31223/osf.io/hvuzy
29. Qi M*, et al.* (2017) Exposure and health impact evaluation based on simultaneous measurement of indoor and ambient PM2.5 in Haidian, Beijing. *Environ. Pollut.* 220:704-712.
30. Chen Y, Ebenstein A, Greenstone M, & Li H (2013) Evidence on the impact of sustained exposure to air pollution on life expectancy from China's Huai River policy. *Proceedings of the National Academy of Sciences* 110(32):12936-12941.
31. Central People's Government of the People's Republic of China (2017) Notice regarding the issuance of Clean Winter Heating Plan in Northern China (2017-2021). http://www.gov.cn/xinwen/2017-12/20/content_5248855.htm.
32. National Energy Administration (2019) Clean heating rate exceeded 5%, https://www.sohu.com/a/362593452_465972.
33. Shi X & Brasseur GP (2020) The Response in Air Quality to the Reduction of Chinese Economic Activities during the COVID‐19 Outbreak. *Geophys. Res. Lett.* doi: https://doi.org/10.1029/2020GL088070.
34. Zhang R*, et al.* (2020) NOx Emission Reduction and Recovery during COVID-19 in East China. *Atmosphere* 11(4):433.
35. Huang T*, et al.* (2017) Spatial and temporal trends in global emissions of nitrogen oxides from 1960 to 2014. *Environ. Sci. Technol.* 51(14):7992-8000.
36. Huang Y*, et al.* (2014) Quantification of Global Primary Emissions of PM2.5, PM10, and TSP from Combustion and Industrial Process Sources. *Environ. Sci. Technol.* 48(23):13834-13843.
37. Shen H*, et al.* (2017) Urbanization-induced population migration has reduced ambient PM 2.5 concentrations in China. *Science Advances* 3(7):e1700300.
38. Shen HZ*, et al.* (2018) Impacts of rural worker migration on ambient air quality and health in China: From the perspective of upgrading residential energy consumption. *Environ. Int.* 113:290-299.
39. Ministry of Environmental Protection (2013) *Exposure Factors Handbook of Chinese Population (Adult volume) (China Environmental Science Press, 2013)*.
40. Zhao S*, et al.* (2019) A Multiphase CMAQ Version 5.0 Adjoint. *Geoscientific Model Development Discussions*. doi: https://doi.org/10.5194/gmd-2019-287.
41. AiMa Forecasts (2020) AiMa air quality forecasting system, http://www.aimayubao.com/wryb_eval.php?movie=no.
42. Lyu B, Zhang Y, & Hu Y (2017) Improving PM2. 5 air quality model forecasts in China using

a bias-correction framework. *Atmosphere* 8(8):147.

43. Energy Statistics Division of National Bureau of Statistics (2018) *China Energy Statistical Yearbook 2018* (China Statistics Press, Beijing, China).
44. US EPA Office of Research and Development (2014) CMAQv5.0.2. doi: https://zenodo.org/record/1079898#.XotQSIhKg2w
45. Skamarock WC, et al. (2008) A description of the advanced research WRF version 3. (National Center For Atmospheric Research Boulder Co Mesoscale and Microscale Meteorology Division).
46. National Centers for Environmental Prediction (2020) NCEP Products Inventory: Global Products, Global Forecast System (GFS) Model. https://www.nco.ncep.noaa.gov/pmb/products/gfs/#GFS
47. Hakami A*, et al.* (2007) The adjoint of CMAQ. *Environ. Sci. Technol.* 41(22):7807-7817.
48. Chen Y*, et al.* (2016) Transition of household cookfuels in China from 2010 to 2012. *Applied Energy* 184:800-809.
49. Johnson M, Lam N, Brant S, Gray C, & Pennise D (2011) Modeling indoor air pollution from cookstove emissions in developing countries using a Monte Carlo single-box model. *Atmos. Environ.* 45(19):3237-3243.
50. World Health Organization (2014) *WHO guidelines for indoor air quality: household fuel combustion – Review 3: Model for linking household energy use with indoor air quality* https://www.who.int/airpollution/guidelines/household-fuel-combustion/Review_3.pdf?ua=1.
51. Xiang J*, et al.* (2019) Reducing Indoor Levels of "Outdoor $PM_{2.5}$" in Urban China: Impact on Mortalities. *Environ. Sci. Technol.* 53(6):3119-3127.
52. Kirkwood TB (1979) Geometric means and measures of dispersion. *Biometrics* 35(4):908-909.
53. Endo Y (2009) Estimate of confidence intervals for geometric mean diameter and geometric standard deviation of lognormal size distribution. *Powder Technol.* 193(2):154-161.
54. Shen HZ*, et al.* (2013) Global Atmospheric Emissions of Polycyclic Aromatic Hydrocarbons from 1960 to 2008 and Future Predictions. *Environ. Sci. Technol.* 47(12):6415-6424.
55. Shi S, Chen C, & Zhao B (2017) Modifications of exposure to ambient particulate matter: Tackling bias in using ambient concentration as surrogate with particle infiltration factor and ambient exposure factor. *Environ. Pollut.* 220:337-347.